International Journal of Cardiology 168 (2013) 3829–3836

Contents lists available at ScienceDirect

International Journal of Cardiology

journal homepage: www.elsevier.com/locate/ijcard

Cell therapy prevents structural, functional and molecular remodeling of remote non-infarcted myocardium ☆

Leonardo dos Santos [a,b,*,1], Giovana A. Gonçalves [b,1], Ana Paula Davel [c,1], Alexandra A. Santos [b,1], José E. Krieger [d,1], Luciana V. Rossoni [e,1], Paulo J.F. Tucci [b,1]

[a] Dept of Physiological Sciences, Federal University of Espirito Santo, Brazil
[b] Dept of Medicine, Federal University of Sao Paulo, Brazil
[c] Dept of Structural and Functional Biology, State University of Campinas, Brazil
[d] Heart Institute, University of Sao Paulo, Brazil
[e] Institute of Biomedical Sciences, University of Sao Paulo, Brazil

ARTICLE INFO

Article history:
Received 23 May 2012
Received in revised form 29 April 2013
Accepted 20 June 2013
Available online 12 July 2013

Keywords:
Myocardial remodeling
Stem-cell
Calcium-handling
Capillary
Hypertrophy

ABSTRACT

Background/objectives: Therapy using bone marrow (BM) cells has been tested experimentally and clinically due to the potential ability to restore cardiac function by regenerating lost myocytes or increasing the survival of tissues at risk after myocardial infarction (MI). In this study we aimed to evaluate whether BM-derived mononuclear cell (MNC) implantation can positively influence the post-MI structural remodeling, contractility and Ca(2+)-handling proteins of the remote non-infarcted tissue in rats.

Methods and results: After 48 h of MI induction, saline or BM-MNC were injected. Six weeks later, MI scars were slightly smaller and thicker, and cardiac dilatation was just partially prevented by cell therapy. However, the cardiac performance under hemodynamic stress was totally preserved in the BM-MNC treated group if compared to the untreated group, associated with normal contractility of remote myocardium as analyzed in vitro. The impaired post-rest potentiation of contractile force, associated with decreased protein expression of the sarcoplasmic reticulum Ca^{2+}-ATPase and phosphorylated-phospholamban and overexpression of Na(+)/Ca(2+) exchanger, were prevented by BM-MNC, indicating preservation of the Ca(2+) handling. Finally, pathological changes on remodeled remote tissue such as myocyte hypertrophy, interstitial fibrosis and capillary rarefaction were also mitigated by cell therapy.

Conclusions: BM-MNC therapy was able to prevent cardiac structural and molecular remodeling after MI, avoiding pathological changes on Ca(2+)-handling proteins and preserving contractile behavior of the viable myocardium, which could be the major contributor to the improvements of global cardiac performance after cell transplantation despite that scar tissue still exists.

1. Introduction

Ischemic heart disease frequently leads to myocardial remodeling and heart failure with impaired life quality, playing an important role in cardiovascular deaths. Due to the impact on public health, experimental therapeutic studies regarding myocardial infarction (MI) and heart failure are often focused. In this way, myocardial implantation of stem cells, such as those derived from the bone marrow (BM), has been tested in both experimental and clinical studies for more than a decade [1,2].

The main mechanism originally proposed for BM-derived cell therapy involved the potential capability to fuse with or differentiate into contractile myocytes and the ability to form new vessels, since adult BM contains pluripotent cell populations [3]. Currently, it has been accepted that tissue regeneration or differentiation plays a minor role, ascribing a major importance to the paracrine-mediated effects on the infarct and border zone by BM-derived stem cells [4].

The functional benefits identified after cell therapy are related to improvement of global cardiac function as assessed by in vivo and in vitro approaches [5–12]. Angiogenesis [8,9,13–15] and reduction of apoptosis [14,16,17] and fibrosis [9,10,12,17] essentially in infarcted and adjacent areas have been reported. Nevertheless, rare information has been provided about remodeling and function of reminiscent and remote regions of the failing left ventricle (LV) after BM-derived cell therapy [7]. In post-MI physiopathology studies, multicellular in vitro preparations of the non-infarcted myocardium allow to evaluate the contractility without influences of the LV fibrotic scar or cavity dimensions, resembling the actual in situ mechanics. In the present study, we

☆ There is no conflict of interest. This work was sponsored by grants-in-aid from Conselho Nacional de Desenvolvimento Científico e Tecnológico (CNPq) and Fundação de Amparo à Pesquisa do Estado de São Paulo (FAPESP).

* Corresponding author at: Departamento de Ciências Fisiológicas, CCS/UFES, Av Marechal Campos 1468, 29043-900 Vitoria-ES, Brazil. Tel./fax: +55 27 3335 7342.
E-mail address: leodossantos@hotmail.com (L. dos Santos).

[1] These authors take responsibility for all aspects of the reliability and freedom from bias of the data presented and their discussed interpretation.

0167-5273/$ – see front matter © 2013 Elsevier Ireland Ltd. All rights reserved.
http://dx.doi.org/10.1016/j.ijcard.2013.06.026

demonstrated that intramyocardial injection of BM-derived mononuclear cells (MNC) in rats reduced infarct size and attenuated structural and functional remodeling of the myocardium remote to the infarct and implantation site, which contributed to the improvement of cardiac performance. In addition, for the first time using BM-MNC in a rodent model of MI, we showed that this approach was associated with preservation of the mechanics of spared myocardium by attenuating deleterious changes on the calcium handling.

2. Material and methods

2.1. Used animals and MI model

Male and female 10–12 week old Lewis inbred rats were used. Animals received humane care and all procedures were in compliance with protocols approved by the Institutional Research Ethics Committee of the Federal University of São Paulo (No. 1468.05). The authors of this manuscript have certified that they comply with the Principles of Ethical Publishing in the International Journal of Cardiology. MI was induced by ligation of the anterior descending coronary artery in 30 female rats as previously described [15,18]. Under anesthesia with ketamine (50 mg/kg) and xylazine (10 mg/kg) intraperitoneally, orotracheal intubation and mechanical ventilation were performed (rodent ventilator, Harvard Apparatus Mod 683; Holliston MA, USA), and through a left thoracotomy the coronary artery was tied with a 6-0 polypropylene suture. The same surgical procedures were performed without coronary occlusion in another 8 rats, named as Sham-operated (Sham) group.

2.2. Isolation and implantation of BM-derived MNC

BM was harvested from male Lewis inbred rats and BM-MNC were isolated as previously reported [15,19]. After the rats were sacrificed, femurs and tibias were excised and placed in phosphate-buffered saline with penicillin G (100 U/ml) and streptomycin (100 μg/ml), and the BM was flushed out of the bones with Dulbecco's modified Eagle's medium. The BM-MNC were isolated by centrifugation through a density-gradient (3:10 Ficoll-Paque Plus; Amersham Biosciences, Uppsala, Sweden) and then suspended in sterile saline. Trypan blue dye (0.4%; Sigma, St. Louis, MO, USA) was used to confirm cell viability, and only samples with viability >90% were used. Forty-eight hours after coronary occlusion, a suspension of 6×10^6 BM-MNC in 100 μl sterile saline (BM-MNC group), or 100 μl of cell-free saline solution (Saline group) was injected into the myocardium at 3 points along the infarct border zone using a 30-gauge needle. The cell and saline injections were performed under direct observation of the LV free wall in open chests to ensure that there was no leakage of solution. Outcome parameters were assessed 6 weeks after coronary occlusion and cell implantation. To evaluate whether injections could deliver BM-MNC in the host ventricle, the Y chromosomes from male donor BM-MNC were searched in the LV sampled from female rats with MI, sacrificed immediately after cell implantation, by using a polymerase chain reaction (PCR). Additionally, implanted cells were also searched in samples collected 6 weeks after surgery. Genomic DNA was extracted and a conventional PCR was performed using primers designed based on a partial sequence of the rat *Sry* gene, which amplify the male sex-determining region on the Y chromosome (forward: 5′-AGT GTT CAG CCC TAC AGC CTG AGG AC-3′ and reverse: 5′-GCT GCA ATG GGA CAA CAA CCT ACA CAC-3′) [15].

2.3. Echocardiography

Infarct size estimation and LV function were evaluated by echocardiography six weeks after MI and BM-MNC therapy. Examination was done by one observer blinded to the animal group, with a HP SONOS 5500 (Philips Medical Systems, Andover, MA, USA) and a 12-MHz/2-cm transducer, according to Santos et al. [18]. The LV end-diastolic and end-systolic transverse areas were measured and fractional area shortening (FAS) was calculated. The parameters of mitral diastolic inflow velocity curves derived from pulsed-wave Doppler (peaks of E- and A-wave velocities) were used to assess diastolic function. The relative infarct extension was measured by echocardiography at basal, middle and apical levels; the length of arc corresponding to the akinetic portion (infarct scar) and the total perimeter of the LV endocardial border were analyzed at the end of diastole; and the relative MI size was expressed as % of the LV transverse perimeter occupied by the infarct averaged in the three planes. Recently, we have shown that this echocardiographic approach provides credible estimates of infarct size that are comparable to histochemical methods [20].

2.4. Direct hemodynamic evaluation

Thereafter, an invasive hemodynamic evaluation was performed using a micromanometer (MikroTip™ 2F; Millar Instruments Inc., Houston, TX, USA) that was inserted into the LV cavity through the carotid artery to measure the intraventricular pressure. Through a brief right thoracotomy, a flow ultrasound probe (Transonic Systems Inc., Ithaca, NY, USA) was positioned around the ascending aorta to estimate LV ejection. Protocols were performed in closed chest anesthetized animals and the following parameters were analyzed: LV systolic and end-diastolic pressures, rate of change of LV pressure, heart rate, cardiac output, stroke volume and stroke work. Stroke work was calculated as the product of stroke volume × (systolic pressure − end-diastolic LV pressure). After evaluation under basal conditions, cardiac performance was tested by acquiring the hemodynamic parameters under a sudden afterload stress, promoted by pressure-overload using a single vasoconstrictive phenylephrine injection (PHE, l-phenylephrine hydrochloride, Sigma, St. Louis, MO, USA). PHE doses were individually adjusted (15–25 μg/kg, intravenously) to produce comparable blood pressure increases of 50–70% over the baseline [21].

2.5. In vitro myocardial contractility

Preparations of isolated LV papillary muscles under isometric contractions were performed as previously described [22]. The heart was quickly removed and the posterior papillary muscle of LV was carefully dissected and vertically mounted in an organ bath heated at 29 °C and 100% oxygenated. Muscle was attached to a force transducer (GRASS FT-03, Astro-Med, Inc., RI, USA) connected to a micrometer for adjustment of muscle length. The composition of the Krebs–Henseleit solution was as follows: (in mM) 135 NaCl; 4.69 KCl; 1.5 CaCl; 1.16 $MgSO_4$; 1.18 KH_2PO_4; 5.50 glucose; 10 U insulin and HEPES 20 buffered at pH 7.3 to 7.4. The preparation was stimulated by platinum electrodes at a frequency of 0.2 Hz, using square-wave pulses of 5-ms duration, and voltage adjusted to a value 10% greater than minimum required producing mechanical response. After 60 min of stabilization at low loading conditions, muscle was loaded to contract isometrically and stretched to peak length of its length–tension curve (L_{max}). Tests were performed at L_{max} (optimum length for contraction), isometric tension was evaluated by force normalized to the muscle cross-sectional area ($g \cdot mm^{-2}$) and the following parameters were obtained: resting tension (RT), peak of developed tension (DT) and its first time derivative (dT/dt), time to peak tension (TPT), time to 50% of relaxation (TR50). Experimental protocol was composed of an analysis of the papillary behavior in: 1) length–tension curves (by stretching muscles from 92 to 100% of L_{max}); 2) relative post-rest contractions (using 6, 10, 15, 30, 45 and 60 s of pause duration); 3) contractile response to calcium (increasing Ca^{2+} concentration from 1.5 to 2.5 mM in bath solution); and 4) contractile response to β-adrenoceptor agonist (adding isoproterenol 5 μM in bath solution).

2.6. Western blotting

Protein expression of sarcoplasmic reticulum Ca^{2+}-ATPase (SERCA2), phospholamban (PLB), phosphorylated phospholamban (Ser^{16}-PLB), α_1 and α_2 isoforms of Na^+, K^+-ATPase (NKA), and Na^+/Ca^{2+}-exchanger (NCX) was analyzed by Western blotting in myocardium microsomal fractions according to previously described [23]. Samples were collected from non-infarcted LV posterior wall and interventricular septum of each experimental group and compared to equal mass of sample from similar LV regions from the Sham group. To prepare the microsomal fractions of proteins, tissue homogenates were centrifuged at 10,000 ×*g* (10 min at 4 °C) followed by an ultra-centrifugation at 100,000 ×*g* (60 min). The pellets, representing the microsomal fraction, were resuspended in Tris–EDTA buffer (in mM: Tris 50, EDTA 1.0, pH = 7.4) and protein concentration was measured by the Bradford's method. Equal protein samples (25 μg) from the reminiscent LV of each group and pre-stained molecular SDS-PAGE standards (Bio-Rad, CA, U.S.A.) were electrophoretically separated on 7.5–12% SDS-PAGEs and then transferred to polyvinyl difluoride membranes overnight at 4 °C, using a Mini Trans-Blot Transfer Cell system (Bio-Rad, CA, U.S.A.). Transferring efficiency and protein charging equality were verified by gel Ponceau S 1% staining (Caledon laboratories, Ontario, Canada) [24]. Then, membranes were blocked (Tris-buffered solution with 5% powdered non-fat milk) and incubated overnight with the following primary monoclonal antibodies: anti-SERCA2 (1:2500, Abcam Inc., MA, USA), anti-PLB (0.25 μg/ml, Upstate Biotechnology, Lake Placid, NY, USA) or anti-phospho-Ser^{16}-PLB (1:1000, Upstate Biotechnology), anti-α_1 Na^+/K^+-ATPase (1:10,000, Upstate Biotechnology), anti-α_2 Na^+/K^+-ATPase (1:5000, Upstate Biotechnology) or anti-NCX1 (1:1500, Swant, Switzerland). After washing, the membranes were incubated with a secondary antibody conjugated to horseradish peroxidase (1:3000, Bio-Rad, CA, USA). The membrane was thoroughly washed and the immunocomplexes were detected using an enhanced horseradish peroxidase/luminol chemiluminescence system (ECL Plus, Amersham International plc, Little Chalfont, UK) and then subjected to autoradiography. Protein blots were quantified by Scion Image software (Scion based on NIH image) in arbitrary units of optical density and normalized by average of values measured for control samples (Sham group) in each membrane.

2.7. Biometry, histology and morphometry

Before the excision of the papillary muscle, the left and right ventricles were weighed separately, in order to use the ventricle mass divided by the body mass as an index suggestive of ventricular hypertrophy. After papillary muscle dissection and LV sample collection for protein assays, the LV samples were anatomically remodeled and fixed in 10% buffered formalin for 24 h, embedded in paraffin, and transversely cut into 3 μm sections. Sections were mounted onto slides and stained with hematoxylin and eosin for myocyte analysis, Picrossirius red for fibrosis evaluation, or periodic acid-Schiff for capillary density quantification. A computerized image acquisition system (Leica Imaging Systems, Bannockburn, IL, USA) was used for the analyses. Histological analysis was performed only in the remote non-infarcted myocardium mainly composed of interventricular septum and posterior wall of the LV. This was used to evaluate tissue remodeling blinded to the experimental group. As an estimative

of myocyte hypertrophy, the average nuclear volume was determined randomly in 50–70 myocytes cut longitudinally for each animal, and calculated according to the following equation: nuclear volume = π × D × d² / 6 where d = shorter nuclear diameter and D = longer nuclear diameter [25]. Fibrosis in the remote non-infarcted LV was considered as the collagen fibers not including stained scars and perivascular fibers. After digitalization, the red-stained areas were quantified as the average percentage of the total area from each of 5 randomized 200× magnification fields per animal. Capillary and myocyte densities were evaluated in 6 randomized 400× magnification fields per animal, where the fibers were cut transversally. Capillarity was expressed as the total amount per area (capillaries/mm²) and as the capillary/myocyte ratio. In addition, the thickness of the scarred myocardial wall was determined in the mid-portion of the infarction in 4 transverse LV histological sections.

2.8. Statistical methods

Student's *t*-test, and one-way ANOVA followed by Tukey's *post hoc* test were used, when appropriate, for statistical analysis of the data. Linear regressions with comparison of its slopes were used to evaluate the papillary length–tension curves. GraphPad Prism 5.0 was used for graphs and statistical analysis. Differences at the *P*-value < 0.05 were considered significant. Results are expressed as mean ± standard error of the mean (SEM).

3. Results

3.1. MI outcomes and BM-MNC implantation

Twenty-seven rats survived coronary occlusion 48 h after surgery, and 22 rats exhibited typical electrocardiographic signs of infarction, as defined by a Q wave in the D1 lead together with ÂQRS and ÂT located between 0 and 240 degrees [26]. The infarcted animals were randomized in Saline ($n = 12$) or BM-MNC ($n = 10$) injections. During the 6-week follow-up, only 1 rat died, from the Saline group.

PCR for *Sry* produced the expected ~400pb fragment in male hearts used as positive controls, but not in female hearts used as negative control. This sequence was also identified in each sample collected immediately and 6 weeks after implantation of male-derived BM-MNC in the female infarcted hearts.

Six weeks after MI production and BM-MNC implantation, the infarct relative size was smaller when compared to the Saline group (Table 1). Furthermore, by transversal planes, the LV scar was longer and thinner in non-treated versus BM-MNC treated animals, suggesting a reduction of infarct expansion (Table 1).

Table 1
Morphologic and functional parameters of experimental groups.

	Sham	Saline	BM-MNC
Biometry			
Body weight (g)	221 ± 9	219 ± 7	196 ± 9
LV wt/body wt ($mg \cdot g^{-1}$)	2.31 ± 0.10	2.97 ± 0.08*	2.62 ± 0.09*,#
RV wt/body wt ($mg \cdot g^{-1}$)	0.64 ± 0.05	1.26 ± 0.08*	0.82 ± 0.03#
PWC (%)	78.76 ± 0.30	81.83 ± 0.29*	79.31 ± 0.27#
Infarct morphology			
Relative size (% LV)	–	44.5 ± 1.4	38.3 ± 1.1#
Scar length (mm)	–	12.3 ± 0.8	9.2 ± 0.4#
Scar thickness (mm)	–	0.63 ± 0.04	0.93 ± 0.04#
Echocardiography			
LVDA (mm^2)	27.4 ± 1.7	58.9 ± 2.5*	40.8 ± 1.9*,#
FAS (%)	59.1 ± 1.1	32.4 ± 1.7*	42.5 ± 1.2*,#
E/A ratio	2.06 ± 0.11	5.29 ± 0.66*	3.26 ± 0.54#
Hemodynamics			
LVSP (mm Hg)	119.1 ± 4.0	107.2 ± 5.5	111.2 ± 4.5
LVEDP (mm Hg)	4.4 ± 0.6	16.3 ± 2.7*	4.9 ± 1.2#
Heart rate (bpm)	358 ± 10	338 ± 13	367 ± 10
$+dP/dt_{max}$ ($mm\ Hg \cdot s^{-1}$)	9635 ± 382	7227 ± 367*	9035 ± 344#
$-dP/dt_{max}$ ($mm\ Hg \cdot s^{-1}$)	−5995 ± 248	−5018 ± 275*	−5774 ± 344#
Cardiac output (ml/min)	49.7 ± 4.4	39.4 ± 4.6	45.6 ± 4.9

Left ventricle (LV); pulmonary water content (PWC); left ventricular diastolic area (LVDA); fractional area shortening (FAS); relation between velocity of E and A waves (E/A ratio); left ventricular systolic (LVSP) and end-diastolic pressures (LVEDP); maximal rate of pressure rise ($+dP/dt_{max}$) and decline ($-dP/dt_{max}$). Sham ($n = 8$); Saline ($n = 11$); BM-MNC ($n = 10$). Values are mean ± SEM.
* $P < 0.05$ vs. Sham.
\# $P < 0.05$ vs. Saline.

3.2. Global cardiac function

Echocardiography revealed chamber dilatation associated with systolic and diastolic dysfunctions in the MI group injected with saline (Table 1). However, therapy with BM-MNC reduced LV dilatation and improved fraction of LV shortening. Also the elevation of E/A ratio was mitigated in the cell-treated rats.

By direct hemodynamic evaluation (Table 1), elevated LV end-diastolic pressure (EDP) and depressed first derivative of pressure ($+dP/dt_{max}$) observed after MI were significantly prevented by BM-MNC injection. Under basal conditions we did not identify significant changes in cardiac output (CO), stroke volume (SV) or stroke work (SW) generation in infarcted rats when compared to Sham.

In the Sham group, response to afterload stress included increment on $+dP/dt_{max}$ and relative maintenance on EDP and SV, associated with SW recruitment (Fig. 1). Conversely, MI untreated rats exhibited elevation on EDP without significant $+dP/dt_{max}$ increase, associated with marked reduction on SV and SW. As shown in Fig. 1, BM-MNC therapy significantly prevented these pathological changes on cardiac performance. Noteworthy, the BM-MNC group increased $+dP/dt_{max}$ and SW, with attenuated fall in LV ejection under afterload stress.

3.3. In vitro myocardial contractility

Typical papillary mechanical recordings are shown in Fig. 2A and measurements under steady state are summarized in Table 2. Both contraction and relaxation parameters, which were impaired in

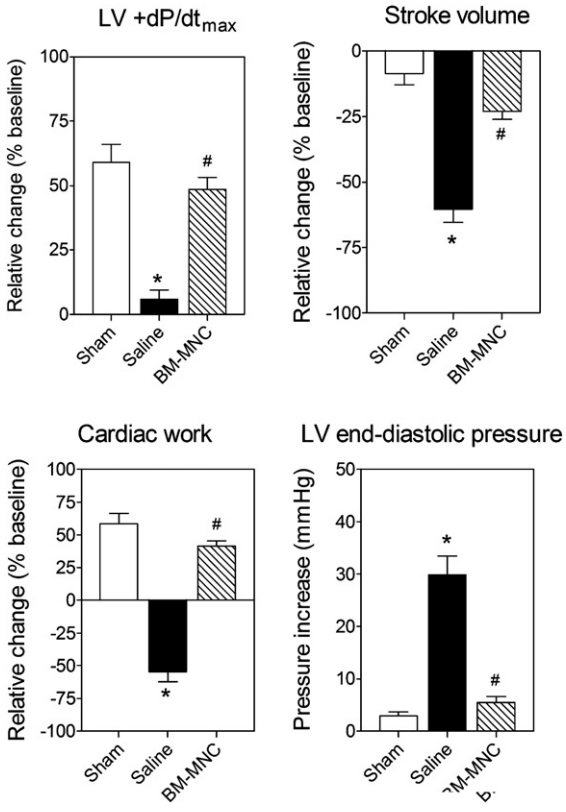

Fig 1. Repercussions induced by sudden afterload stress in LV maximal rate of pressure rise ($+dP/dt_{max}$); stroke volume; cardiac work and LV end-diastolic pressure. Positive or negative values result from relative increase or decrease on that parameter. Sham ($n = 8$); Saline ($n = 7$); BM-MNC ($n = 7$). Values are means ± SEM. *$P < 0.05$ vs. Sham; #$P < 0.05$ vs. Saline.

infarcted group receiving Saline, were significantly preserved in the BM-MNC group (Table 2). Inotropic responses to increased extracellular calcium or isoproterenol (Fig. 2B and C, respectively) were significantly depressed in the Saline group, but in the BM-MNC treated group the force gain was equivalent to Sham. In response to stretching (Fig. 2D), the best fitting of the length–tension relation (linear regression) resulted in lower slope in Saline (0.12 ± 0.02 g·mm^{-2}/% L_{max}) if compared to Sham (0.29 ± 0.01), and apparently normal in the BM-MNC group (0.25 ± 0.02) (Fig. 2E); regarding the relation between stretching and passive tension, Neperian logarithm transformations of RT values were needed to better fit on linear regressions (Fig. 2F). As a result, only slopes from Saline injected group (0.20 ± 0.02 $\log_n$[RT] / % L_{max}) were higher than others (Sham: 0.15 ± 0.01; BM-MNC: 0.14 ± 0.01) suggesting an increased stiffness. As shown in Fig. 3A, the post-rest contraction protocol evidenced that the papillary muscles from Sham rats exhibit potentiation proportional to the pause period. This phenomenon, which allows to indirectly evaluate sarcoplasmic reticulum function and calcium handling, was significantly depressed in Saline but preserved in the BM-MNC group (Fig. 3B).

Table 2
Papillary muscle mechanics under isometric contraction.

	Sham	Saline	BM-MNC
Developed tension (g·mm^{-2})	6.07 ± 0.32	2.98 ± 0.26*	5.64 ± 0.41#
Resting tension (g·mm^{-2})	1.10 ± 0.11	1.39 ± 0.12	1.17 ± 0.10
$+dT/dt_{max}$ (g·mm^{-2}·s^{-1})	51.4 ± 2.4	26.5 ± 2.3*	46.5 ± 3.1#
$-dT/dt_{max}$ (g·mm^{-2}·s^{-1})	−21.8 ± 1.4	−11.6 ± 1.3*	−19.9 ± 1.8#
TPT (ms)	169 ± 12	220 ± 9*	189 ± 9
TR50 (ms)	156 ± 8	226 ± 16*	180 ± 10#

Maximum rate of tension development ($+dT/dt_{max}$) and decline ($-dT/dt_{max}$); time to peak tension (TPT) and time to 50% relaxation (TR50). Sham ($n = 7$); Saline ($n = 6$); BM-MNC ($n = 7$). Values are means ± SEM.
* $P < 0.05$ vs. Sham.
\# $P < 0.05$ vs. Saline.

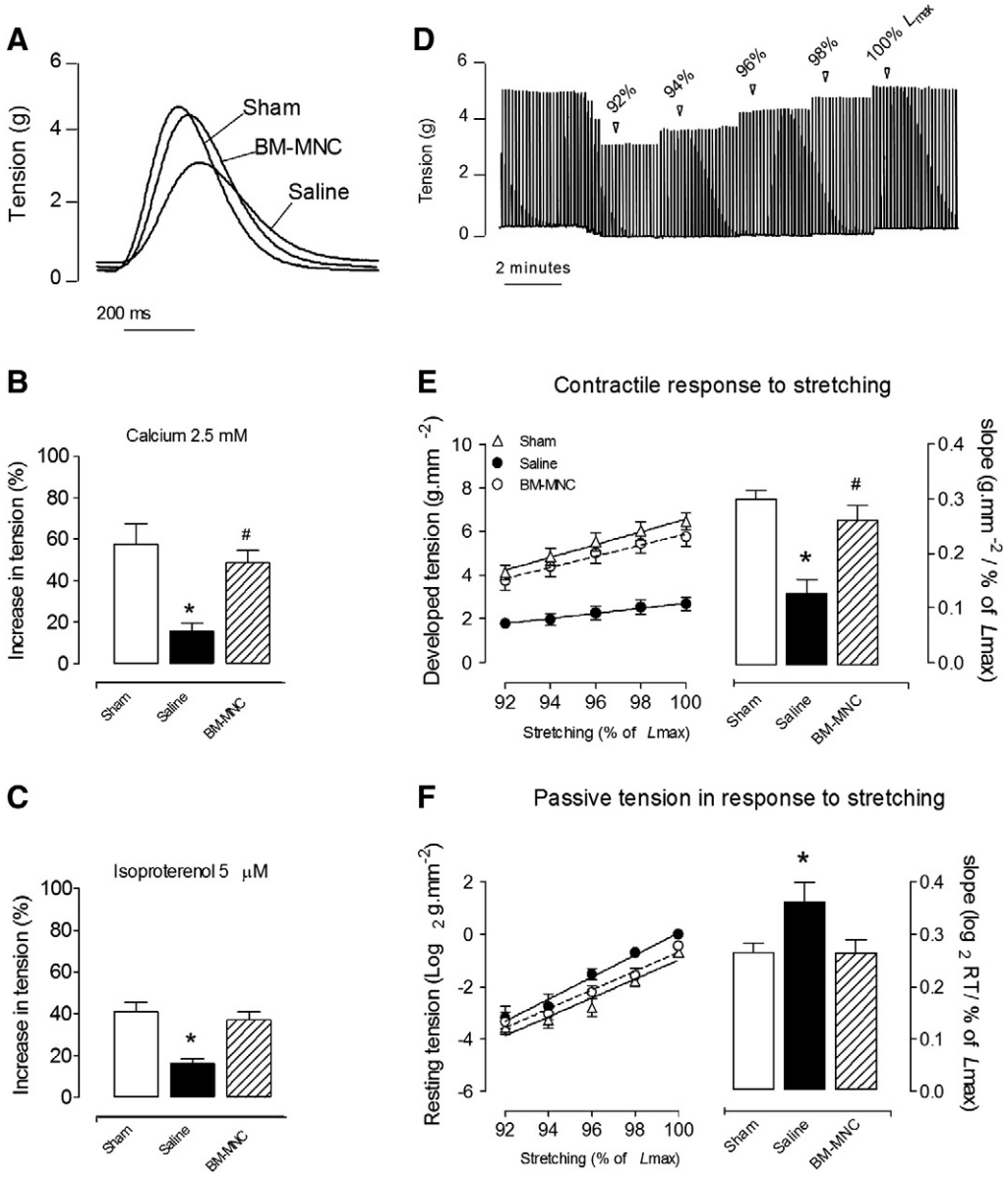

Fig. 2. In panel A: Original representative recordings of papillary muscles isolated from a Sham-operated rat (Sham), a post-MI injected with cell-free saline solution (Saline), and a post-MI transplanted with bone marrow cells (BM-MNC). Inotropic response to increased Ca^{2+} (B) or isoproterenol (C) on bath solution. Example record of a stretch–tension protocol (D) and summary data of developed tension (E) and passive tension (F) in response to stretching. Bars represent slopes of the linear regressions. Sham ($n = 7$); Saline ($n = 6$); BM-MNC ($n = 7$). Values are means ± SEM. *$P < 0.05$ vs. Sham; #$P < 0.05$ vs. Saline.

3.4. Calcium handling proteins

Western blot analysis (Fig. 4) showed that post-MI remodeled myocardium from the Saline group contained lower levels of SERCA2, total and phosphorylated PLB when compared to Sham, supporting an impaired SR Ca^{2+} uptake function. Furthermore, NCX was overexpressed in LV from infarcted rats. Nevertheless, these changes were significantly prevented in BM-MNC treated hearts that exhibited SERCA2, PLB and NCX contents very similar to Sham. While α_1 isoform of NKA remained unchanged in all groups, the diminished content of α_2-NKA in the Saline group was not prevented by the BM-MNC therapy.

3.5. Biometry and morphometry

Cardiac masses are presented in Table 1. Although the body mass was similar between the groups, the LV and RV masses as a function of body mass in the Saline group were significantly increased when compared to Sham, while the group receiving BM-MNC had these parameters preserved. Histological analysis on the remodeled myocardium remote to the infarct showed a significant increase in the myocyte nuclei volume estimated in Saline injected hearts, which was partially prevented by BM-MNC (Fig. 5G). As a result, the myocyte density in the Saline group was lower than Sham and BM-MNC (Fig. 5H). In addition, cardiac tissues from Saline group exhibited low capillary densities and capillary/myocyte ratio, while BM-MNC therapy normalized these parameters (Fig. 5I–J and representative microphotographs in 5A–C). Interstitial collagen was increased in the Saline but apparently normal in the BM-MNC group (Fig. 5K, representative microphotographs are in 5D–F).

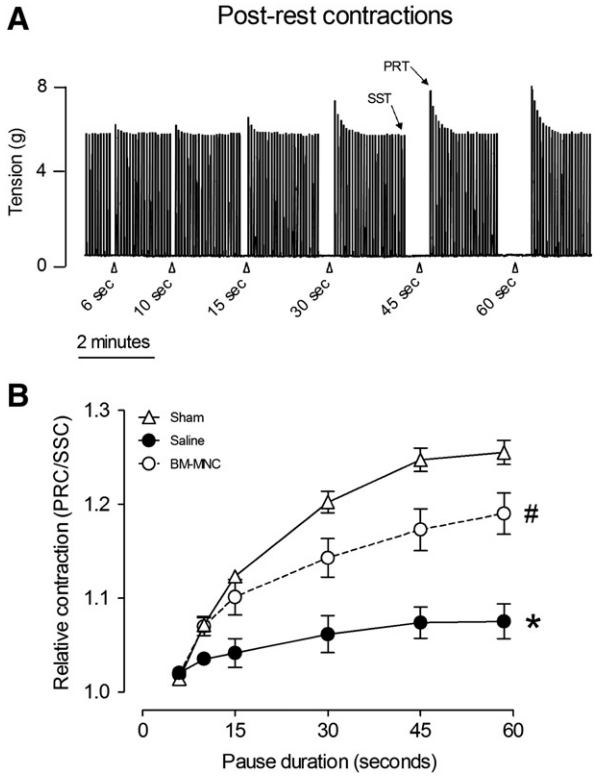

Fig. 3. In panel A: Example record of post-rest potentiation protocol in papillary muscle isolated from a Sham-operated rat. Arrow heads indicate the pauses of stimulation. In B: Effect of increasing pause durations on the relative contraction PRC/SSC (post-rest divided by steady state contraction). Sham ($n = 7$); Saline ($n = 6$); BM-MNC ($n = 7$). Values are means ± SEM. $^{*}P < 0.05$ vs. Sham; $^{\#}P < 0.05$ vs. Saline.

4. Discussion

Cell therapies for cardiac repair are mainly aimed to reduce infarct damage and finally attenuate the dysfunction associated to pathological remodeling. In the present study, we confirmed that intramyocardial injection of BM-MNC in rats, 48 h after coronary occlusion, can reach this goal, since this therapy reduced infarct size and reduced cardiac dysfunction and lung congestion. Although the exact mechanisms are not completely understood, here we credited it to an improvement of the contractility of remote non-infarcted myocardium after BM-MNC therapy, restored expression of proteins involved in calcium mobilization, preserved capillarity and reduced interstitial fibrosis and myocyte hypertrophy.

The effectiveness of BM-MNC injections was confirmed by detection of the *Sry* gene from male cells in host female samples collected immediately after implantation. Compared to other routes of injection, we previously demonstrated that intramyocardial delivery is more efficient for cell survival and cardiac retention, which potentiated its beneficial effects in the ischemic myocardium [19]. Although conventional PCR does not allow estimation of cell engraftment, a long-term permanence of implanted cells seems to be irrelevant, since the current literature distrusts a direct regenerative capability of these BM-derived cells [5,17,27]. Independent of the mechanism, i.e. regenerative or paracrine, the number of transplanted cells in the host tissue, at the adequate therapeutic window, such as the acute phase, is rationally critical for cardiac applications including in patients [28].

Our echocardiographic and hemodynamic data corroborate previous findings of BM-MNC related benefits regarding cardiac dilatation and dysfunction [5,8,11,13,17,27,29,30]. These positive outcomes have been credited to the ability of the implanted cells in reducing ischemia and necrosis, and/or regenerating lost tissue; anyway, diminishing the infarct extension [5,8,11,13,31]. Nevertheless, despite the sizeable scars remaining in the infarcted rats receiving BM-MNC, there was a surprisingly effective response under sudden afterload hemodynamic stress, comparable to Sham. As a result, this remarkable effect should not be credited only to reduced MI scar. In previous works, we have proposed this hemodynamic stress test as a practical method to evaluate cardiac performance in rats, which primarily depends on: i) LV chamber size; ii) response to myocardial stretch; and iii) the intrinsic myocardial contractility [19,21]. Since BM-MNC therapy partially reduced the post-MI ventricular dilatation, the adequate cardiac performance could be attributed, at least in part, to this benefit on chamber size. In addition, effects on other components of this response were clearly evidenced. While cardiac muscle isolated from infarcted group exhibited depressed response to stretching, suggesting that Frank–Starling mechanism was impaired or exhausted, cell therapy significantly preserved it. Moreover, contractility of the reminiscent myocardium was also preserved by cell therapy, including inotropic responses to β adrenoceptor stimulation. Because cardiomyocyte dysfunction is recurrently ascribed to changes on Ca^{2+}-handling [32], we also intend to investigate whether BM-MNC therapy could preserve the mechanics of remote non-infarcted myocardium by ameliorating the SR function and modulating the main Ca^{2+}-handling proteins. The contractile response to rest of stimulation and to increasing Ca^{2+}, which indirectly evaluates excitation–contraction coupling [33], was substantially depressed in the MI group. Supporting this functional data, we observed here a significant reduction on protein content of SERCA2, PLB-Ser^{16} and α_2-NKA, and an overexpression of NCX. While the impaired SR Ca^{2+} uptake contributes to defective storing function, the overexpressed NCX with reduced α_2-NKA intensifies the Ca^{2+} withdrawn through the membrane [34]. In the BM-MNC group, post-rest potentiations and Ca^{2+}-handling protein expression on remote non-infarcted myocardium were substantially normalized, despite of no effects on α_2-NKA isoform, suggesting effects on specific molecular targets.

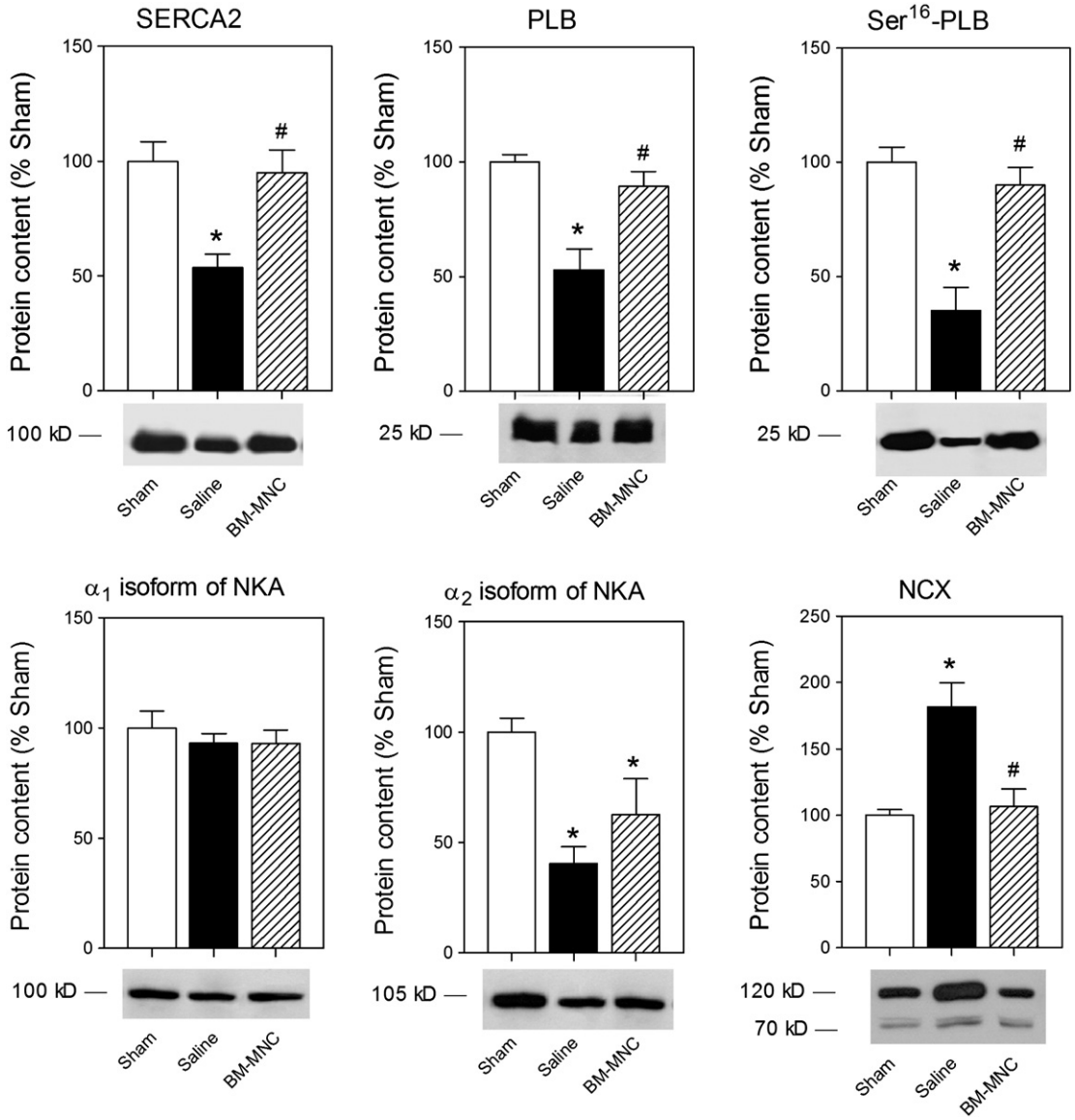

Fig. 4. Protein content of sarcoplasmic reticulum Ca^{2+}-ATPase (SERCA2), phospholamban (PLB), phosphorylated phospholamban (Ser^{16}-PLB), α_1 and α_2 isoforms of Na^+, K^+-ATPase (NKA), and Na^+/Ca^{2+}-exchanger (NCX) on microsomal fractions of reminiscent myocardium from experimental groups. Sham ($n = 6$); Saline ($n = 6$); BM-MNC ($n = 6$). Bars are means ± SEM, and lower pictures are example Western blots. $^*P < 0.05$ vs. Sham; $^\#P < 0.05$ vs. Saline.

Moreno-Gonzales et al. described that cell therapy can enhance Ca^{2+} sensitivity of the remote myocardium without effects on myosin and troponin isoforms [6] indicating a modulation on the Ca^{2+}-handling. In addition, Lee et al., by using BM-MNC or skeletal myoblasts, identified that the impaired Ca^{2+} transient and the SR Ca^{2+} leak observed in failing cardiomyocytes were normalized after therapy, although varying with the type of cell used [7]. Taking together, because the BM-MNC therapy mitigated the contractile dysfunction and preserved the Frank–Starling mechanism of the remnant cardiac muscle, the improved LV performance is reasonable and physiologically supported.

Similar to what was observed in our results, the post-MI remodeling is constantly evidenced in the reminiscent LV tissue [35,36]. Regarding the BM-MNC effects, the biometrical and histological indications of myocardial hypertrophy were partially prevented in rats receiving BM-MNC, as well as changes on capillarity and collagen deposition on the remote tissue.

Injection of BM-derived cells can indeed lead to less fibrosis in both the border zones and adjacent areas [10,11] probably due to paracrine modulation of cardiac fibroblasts [12,37]. According to what was presented here, also in the myocardium remote to infarct/healing regions BM-MNC therapy significantly mitigated interstitial fibrosis, being the structural substrate by which the cell therapy restrained the diastolic dysfunction and preserved the passive mechanical properties of the surviving muscle. In addition, vascular neoformation has been the most studied effect involving stem cell therapy for MI, being a consensus that BM-MNC plays a paracrine-mediated action on the border zone microvasculature rather than differentiates in vascular cells [5,13,14,31]. Once again, few authors have studied the myocardium remote to implant [31]. Here we have presented positive long-term effects of BM-MNC on the microvasculature in a site where the presence of injected cells is unlikely, which reinforces an indirect effect. This preservation of capillarity on reminiscent myocardium could support tissue perfusion and prevent ischemic episodes, arrhythmias, and finally contractile dysfunction.

Actually, we previously reported that the primary benefit from implanted BM-MNC may be improving border zone healthy and reducing infarct expansion, therefore preventing wall thinning and

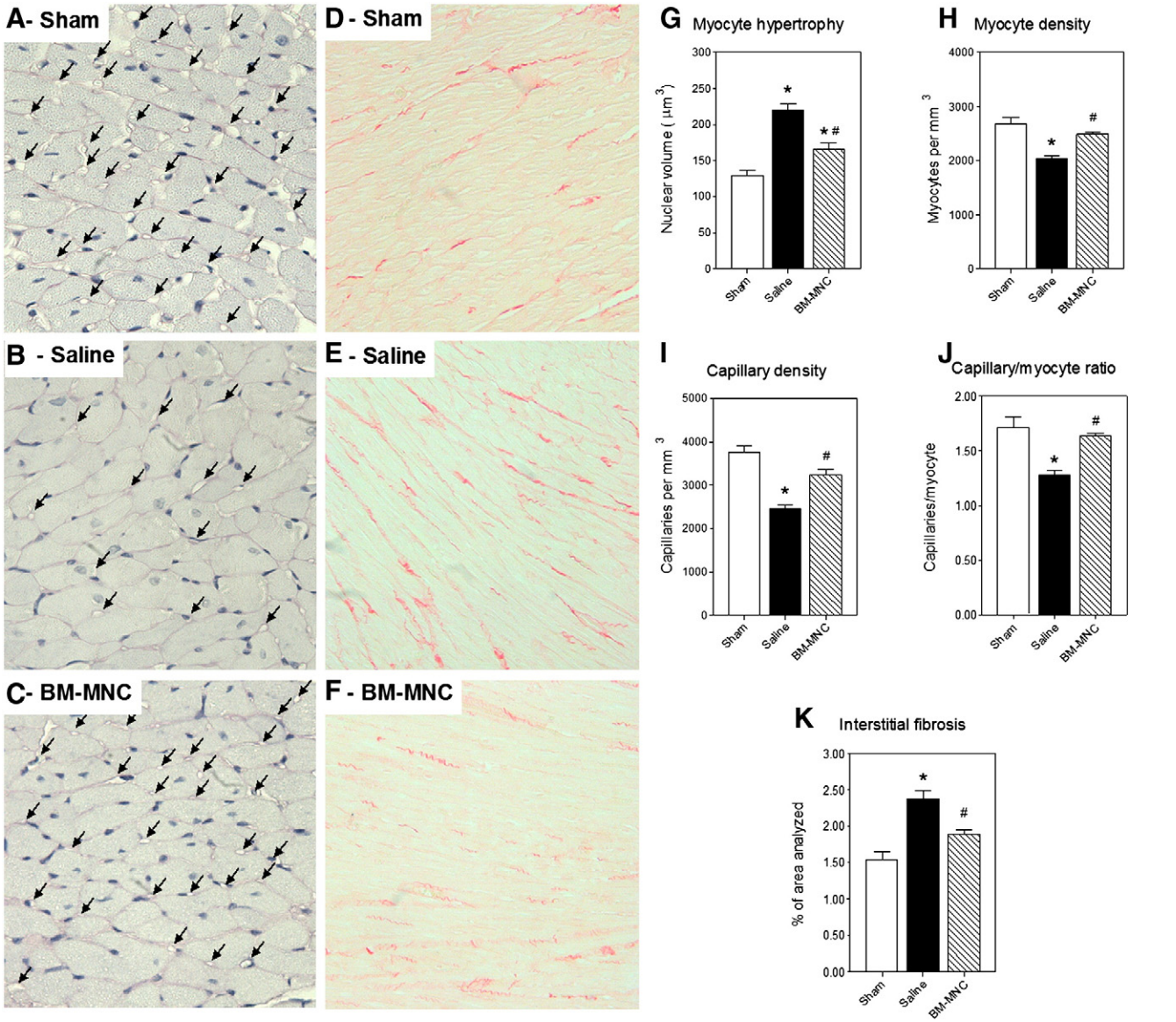

Fig. 5. Representative microphotographs of the remote remodeled myocardium stained with (A–C) Periodic acid-Schiff for capillary counting (400× original magnification, arrows indicate some capillaries), and (D–F) eosin–Picrossirius red for interstitial fibrosis evaluation (200× original magnification). Remodeling parameters including myocyte hypertrophy (G–H), capillarity (I–J), and interstitial fibrosis (K) were evaluated in remote myocardial samples from experimental groups. Bars are means ± SEM. $^{*}P < 0.05$ vs. Sham; $^{\#}P < 0.05$ vs. Saline.

scar dyskinesis, and consequently sustaining that effect observed on systolic function [15]. As also proposed by Moreno-Gonzales et al. [6], a possible explanation is that injected BM-MNC could play beneficial paracrine actions on the infarct and border zones by reducing ischemia, limiting myocyte death and providing neoangiogenesis and, therefore, reducing global load of the heart and attenuating those structural and molecular changes related to myocardial remodeling.

In summary, our study indicates that this therapy provides significant benefits facing the structural remodeling of that reminiscent tissue, such as decreasing interstitial fibrosis and normalizing capillarity, which could contribute to adequate ventricular compliance and perfusion. Furthermore, cell transplantation perhaps also influence cardiomyocyte remodeling, preserving its contractile response by mitigating maladaptive changes on the Ca^{2+}-handling protein profile. Thus, we have presented evidences that BM-MNC implantation improves cardiac function, associated with reduced pathological remodeling of the viable myocardium remote to an infarct in rats, reinforcing its therapeutic potential for ischemic cardiac repair.

Acknowledgments

Special acknowledgment is given to Ednei L. Antonio for surgical assistance, and to Marcio Chaves for preparation of histology slides.

References

[1] Strauer BE, Steinhoff G. 10 years of intracoronary and intramyocardial bone marrow stem cell therapy of the heart: from the methodological origin to clinical practice. J Am Coll Cardiol 2011;58(11):1095–104.
[2] Wollert K, Drexler H. Cell-based therapy for heart failure. Curr Opin Cardiol 2006;21(3):234–9.
[3] Orlic D, Hill JM, Arai AE. Stem cells for myocardial regeneration. Circ Res 2002;91(12):1092–102.
[4] Segers VFM, Lee RT. Stem-cell therapy for cardiac disease. Nature 2008;451(7181):937–42.
[5] Iso Y, Spees JL, Serrano C, et al. Multipotent human stromal cells improve cardiac function after myocardial infarction in mice without long-term engraftment. Biochem Biophys Res Commun 2007;354(3):700–6.
[6] Moreno-Gonzalez A, Korte FS, Dai J, et al. Cell therapy enhances function of remote non-infarcted myocardium. J Mol Cell Cardiol 2009;47(5):603–13.

[7] Lee J, Stagg MA, Fukushima S, et al. Adult progenitor cell transplantation influences contractile performance and calcium handling of recipient cardiomyocytes. Am J Physiol Heart Circ Physiol 2009;296(4):H927–36.
[8] Nagaya N, Fujii T, Iwase T, et al. Intravenous administration of mesenchymal stem cells improves cardiac function in rats with acute myocardial infarction through angiogenesis and myogenesis. Am J Physiol Heart Circ Physiol 2004;287(6):H2670–6.
[9] Liu J, Wang B, Hung H, Chang H, Shyu K. Human mesenchymal stem cells improve myocardial performance in a splenectomized rat model of chronic myocardial infarction. J Formos Med Assoc 2008;107(2):165–74.
[10] Guo J, Lin G-s, Bao C-y, Hu Z-m, Hu M-y. Anti-inflammation role for mesenchymal stem cells transplantation in myocardial infarction. Inflammation 2007;30(3):97–104.
[11] Xu X, Xu Z, Xu Y, Cui G. Selective down-regulation of extracellular matrix gene expression by bone marrow derived stem cell transplantation into infarcted myocardium. Circ J 2005;69(10):1275–83.
[12] Wang Y, Hu X, Xie X, He A, Liu X, Wang J-a. Effects of mesenchymal stem cells on matrix metalloproteinase synthesis in cardiac fibroblasts. Exp Biol Med 2011;236(10):1197–204.
[13] Tang YL, Zhao Q, Qin X, et al. Paracrine action enhances the effects of autologous mesenchymal stem cell transplantation on vascular regeneration in rat model of myocardial infarction. Ann Thorac Surg 2005;80(1):229–37.
[14] Uemura R, Xu M, Ahmad N, Ashraf M. Bone marrow stem cells prevent left ventricular remodeling of ischemic heart through paracrine signaling. Circ Res 2006;98(11):1414–21.
[15] dos Santos L, Santos AA, Gonçalves GA, Krieger JE, Tucci PJF. Bone marrow cell therapy prevents infarct expansion and improves border zone remodeling after coronary occlusion in rats. Int J Cardiol 2010;145(1):34–9.
[16] Tang YL, Zhao Q, Zhang YC, et al. Autologous mesenchymal stem cell transplantation induce VEGF and neovascularization in ischemic myocardium. Regul Pept 2004;117(1):3–10.
[17] Berry MF, Engler AJ, Woo YJ, et al. Mesenchymal stem cell injection after myocardial infarction improves myocardial compliance. Am J Physiol Heart Circ Physiol 2006;290(6):H2196–203.
[18] Santos AA, Helber I, Flumignan RLG, et al. Doppler echocardiographic predictors of mortality in female rats after myocardial infarction. J Card Fail 2009;15(2):163–8.
[19] Nakamuta JS, Danoviz ME, Marques FLN, et al. Cell therapy attenuates cardiac dysfunction post myocardial infarction: effect of timing, routes of injection and a fibrin scaffold. PLoS One 2009;4(6):e6005.
[20] dos Santos L, Mello AFS, Antonio EL, Tucci PJF. Determination of myocardial infarction size in rats by echocardiography and tetrazolium staining: correlation, agreements, and simplifications. Braz J Med Biol Res 2008;41(3):199–201.
[21] dos Santos L, Antonio EL, Souza AFM, Tucci PJF. Use of afterload hemodynamic stress as a practical method for assessing cardiac performance in rats with heart failure. Can J Physiol Pharmacol 2010;88(7):724–32.
[22] Antonio EL, Dos Santos AA, Araujo SRR, et al. Left ventricle radio-frequency ablation in the rat: a new model of heart failure due to myocardial infarction homogeneous in size and low in mortality. J Card Fail 2009;15(6):540–8.
[23] Rossoni LV, Xavier FE, Moreira CM, et al. Ouabain-induced hypertension enhances left ventricular contractility in rats. Life Sci 2006;79(16):1537–45.
[24] Romero-Calvo I, Ocón B, Martínez-Moya P, et al. Reversible Ponceau staining as a loading control alternative to actin in Western blots. Anal Biochem 2010;401:318–20.
[25] Gerdes A, Liu Z, Zimmer H. Changes in nuclear size of cardiac myocytes during the development and progression of hypertrophy in rats. Cardioscience 1994;5(3):203–8.
[26] Bonilha AMM, Saraiva RM, Kanashiro RM, Portes LA, Antonio EL, Tucci PJF. A routine electrocardiogram cannot be used to determine the size of myocardial infarction in the rat. Braz J Med Biol Res 2005;38:615–9.
[27] Limbourg F, Ringes-Lichtenberg S, Schaefer A, et al. Haematopoietic stem cells improve cardiac function after infarction without permanent cardiac engraftment. Eur J Heart Fail 2005;7(5):722–9.
[28] Miettinen JA, Ylitalo KV, Niemelä M, et al. Left ventricular functional recovery after intracoronary injection of autologous bone marrow-derived stem cells in patients with acute myocardial infarction: a dose-response pilot study. Int J Cardiol 2012;154(3):354–6.
[29] Templin C, Kotlarz D, Marquart F, et al. Transcoronary delivery of bone marrow cells to the infarcted murine myocardium. Basic Res Cardiol 2006;101(4):301–10.
[30] Yip H-K, Chang L-T, Wu C-J, et al. Autologous bone marrow-derived mononuclear cell therapy prevents the damage of viable myocardium and improves rat heart function following acute anterior myocardial infarction. Circ J 2008;72(8):1336–45.
[31] Hiasa K-i, Egashira K, Kitamoto S, et al. Bone marrow mononuclear cell therapy limits myocardial infarct size through vascular endothelial growth factor. Basic Res Cardiol 2004;99(3):165–72.
[32] Gomez AM, Guatimosim S, Dilly KW, Vassort G, Lederer WJ. Heart failure after myocardial infarction: altered excitation–contraction coupling. Circulation 2001;104(6):688–93.
[33] Mill J, Vassallo D, Leite C. Mechanisms underlying the genesis of post-rest contractions in cardiac muscle. Braz J Med Biol Res 1992;25(4):399–408.
[34] Bocalini DS, dos Santos L, Antonio EL, et al. Myocardial remodeling after large infarcts in rat converts post rest-potentiation in force decay. Arq Bras Cardiol 2012;98(3):243–51.
[35] Swynghedauw B. Molecular mechanisms of myocardial remodeling. Physiol Rev 1999;79(1):215–62.
[36] Mill JG, Stefanon I, dos Santos L, Baldo MP. Remodeling in the ischemic heart: the stepwise progression for heart failure. Braz J Med Biol Res 2011;44:890–8.
[37] Mias C, Lairez O, Trouche E, et al. Mesenchymal stem cells promote matrix metalloproteinase secretion by cardiac fibroblasts and reduce cardiac ventricular fibrosis after myocardial infarction. Stem Cells 2009;27(11):2734–43.